

INEEL/CON-03-01264
PREPRINT

RELAP5/MOD3.2 Assessment Using INSC SP-PSBV1

P. D. Bayless (INEEL)
O. Melikhov (EREC)
V. Melikhov (EREC)
Yu. Parfenov (EREC)
O. Gavritenkova (EREC)
I. Elkin (EREC)
I. Lipatov (EREC)

October 28, 2003 – October 30, 2003

Seventh International Information Exchange Forum on "Safety Analysis for Nuclear Power Plants of VVER and RBMK Types" (Forum-7)

This is a preprint of a paper intended for publication in a journal or proceedings. Since changes may be made before publication, this preprint should not be cited or reproduced without permission of the author.

This document was prepared as a account of work sponsored by an agency of the United States Government. Neither the United States Government nor any agency thereof, or any of their employees, makes any warranty, expressed or implied, or assumes any legal liability or responsibility for any third party's use, or the results of such use, of any information, apparatus, product or process disclosed in this report, or represents that its use by such third party would not infringe privately owned rights. The views expressed in this paper are not necessarily those of the U.S. Government or the sponsoring agency.

RELAP5/MOD3.2 Assessment Using INSC SP-PSBV1

P. Bayless, INEEL

O. Melikhov, V. Melikhov, Yu. Parfenov, O. Gavritenkova, I. Elkin, I. Lipatov, EREC

October 2003

Abstract

Assessments of the RELAP5/MOD3.2 computer code using loss-of-coolant experiment data from the PSB facility have been performed independently by analysts at the Electrogorsk Research and Engineering Center and the Idaho National Engineering and Environmental Laboratory. The PSB experiment facility is a full height, 1/300 volume and power scale representation of a VVER-1000 reactor. The experiment modeled was an 11% break in the upper plenum, simulating the rupture of one of the hydroaccumulator injection lines. The two assessments were compared, investigating differences in the input models and explaining the resultant differences in the calculations. Both calculations agreed reasonably well with most of the significant phenomena occurring during the test. Both teams concluded that there was only minimal agreement between the calculated and measured mixture level and entrainment in the core. Some changes in input modeling can improve the prediction of the core void distribution. Application of these findings to the full size plant need to consider that PSB has only one simulated fuel bundle, and as a result there may be scaling issues that need to be addressed.

Introduction

RELAP5/MOD3.2¹ code assessment calculations of VVER Standard Problem PSBV1² have been performed independently by analysts at the Electrogorsk Research and Engineering Center (EREC) and the Idaho National Engineering and Environmental Laboratory (INEEL). The PSB experiment analyzed represented an 11% break in the upper plenum region of the reactor vessel, simulating the rupture of one of the hydroaccumulator injection lines. The assessment results were compared to determine how differences in modeling approaches and user input options might affect the transient simulation. These assessments aid in determining the applicability of RELAP5/MOD3.2 for analyzing transients in VVER-type reactors.

PSB Facility Description

The PSB-VVER facility (see Figure 1) is a full-height scale model of a VVER-1000 reactor that is approximately 1/300 scale in volume and power. The facility has four coolant loops. The pressurizer surge line is connected to two of the hot legs, with only one flow path being used in a given experiment. Emergency core coolant (ECC) injection is provided by four hydroaccumulators and by an active pump simulating the high- and low-pressure injection system pumps. All system components are insulated from the environment with glass wool insulation, but during initial steady state operation about 3.4% of the input heat is lost to the environment.

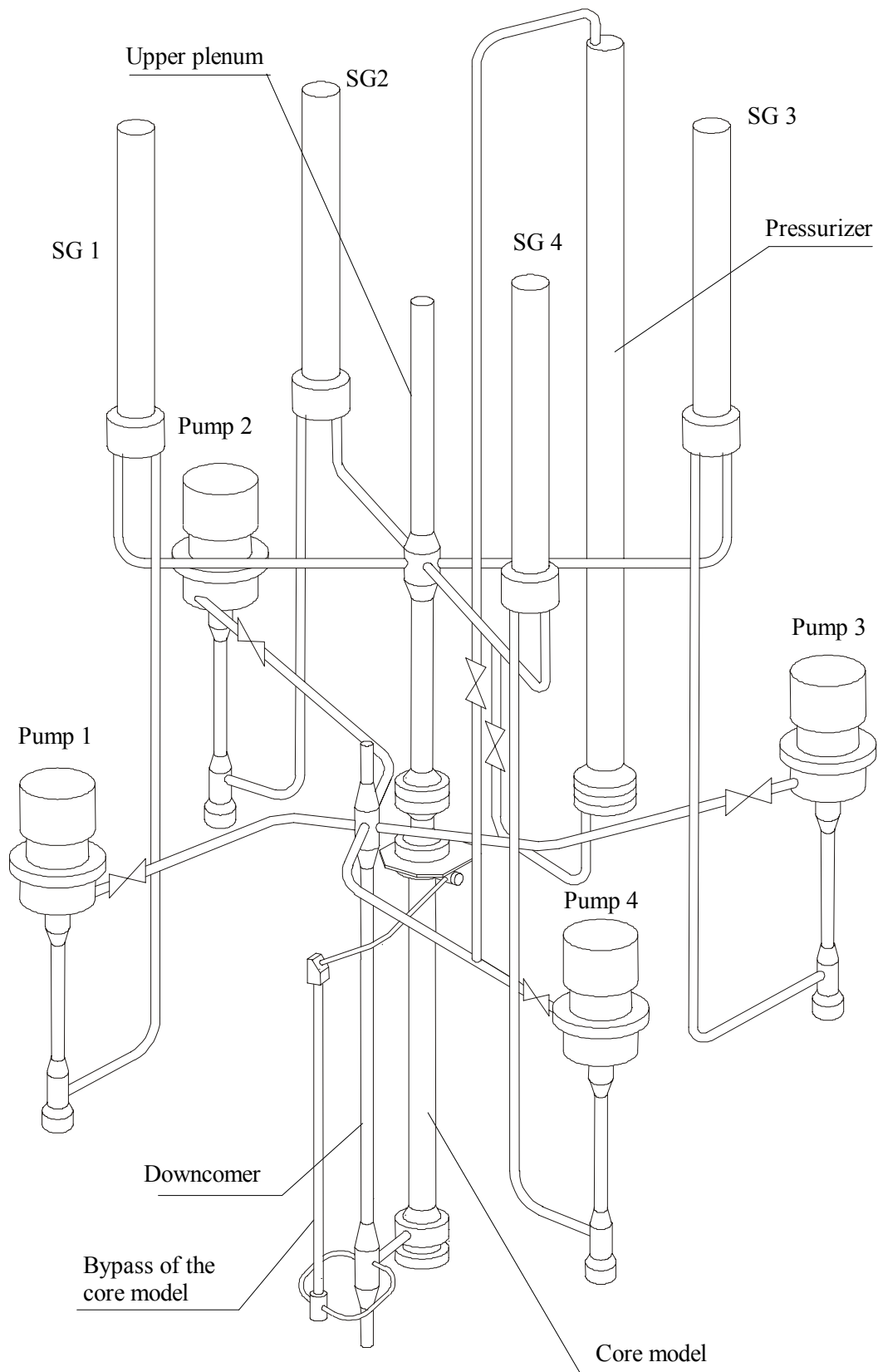


Figure 1. Schematic diagram of the PSB-VVER facility.

The internals of the VVER vessel are represented in the facility by separate pipes for the downcomer, the core and upper plenum, and the core bypass. A horizontal pipe connects the lower portion of the downcomer to the core and core bypass pipes. There is also a small pipe connecting the top of the downcomer to the upper plenum. The core contains 168 full height hollow fuel rod simulators (hereinafter, heater rods) with a uniform power profile and a center unheated rod. About 3% of the downcomer flow is diverted through the core bypass instead of going through the core. Special flow restrictors, each consisting of a plate with two holes of 7 mm diameter, were inserted at either end of the core bypass section. The bypass section is heated over the same elevation range as the core but only receives about 1% of the core power.

Each coolant loop includes a hot leg, steam generator, pump suction piping, pump, and cold leg. The primary side of each steam generator contains hot and cold collectors, and 27 steam generator tubes. Each tube is a coil with ten complete turns, inclined slightly downward from the hot collector to the cold collector. The secondary side has a feedwater ring in the plenum above the steam generator tubes, and no separate downcomer region. The four steam generators are connected to a common steam header. Feedwater flow to the steam generators is not continuous. Flow is provided when needed to keep the water level within the desired operating band.

The break was located in a special pipe connected to the upper plenum. An insert with an inner diameter of 16 mm and a length-to-diameter ratio of 10 was installed in the 45-mm diameter break piping. A valve downstream of the insert was opened to initiate the transient.

Cylinders in the downcomer and upper plenum are used to separate the ECC flows from the break and the hot and cold leg nozzles. The break piping and hot and cold legs are connected to the outer walls of the upper plenum and downcomer. The emergency core cooling system (ECCS) piping is connected to the inside of these cylinders, providing a barrier to immediate bypass of the ECC flow into the loop piping or out the break.

RELAP5 Input Model Descriptions

RELAP5/MOD3.2 input models were developed by the EREC and INEEL analysts to simulate the experiment. All of the major features of the experiment facility were included in both input models. Each of the four coolant loops included a hot leg, steam generator, pump suction loop seal piping, main coolant pump, and a cold leg. The downcomer, core, core bypass, and upper plenum were also included in the model. The pressurizer was modeled. High pressure injection flow was provided to the loop 4 hot leg, and four hydroaccumulators provided flow to the downcomer and upper plenum (two to each location). Nodalization diagrams for the EREC model are shown in Figures 2-4. The nodalizations of the other coolant loops and steam generators are similar to those shown in Figures 3 and 4. Figure 5 provides a nodalization diagram for the INEEL model, showing the reactor vessel components and one coolant loop with the pressurizer; the other three loops have identical nodalizations, except that two loops are not connected to the pressurizer.

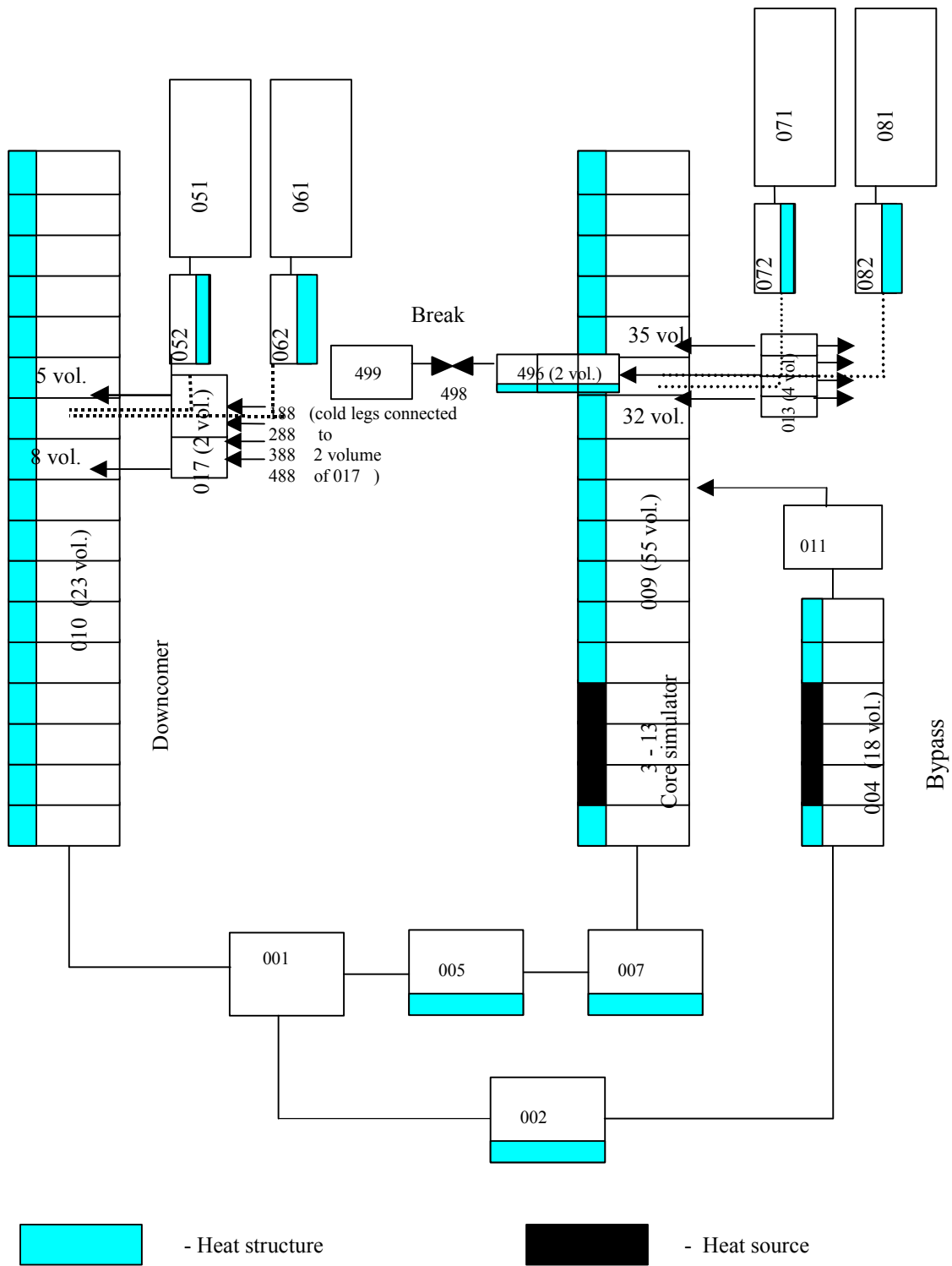


Figure 2. EREC nodalization of the core and core bypass.

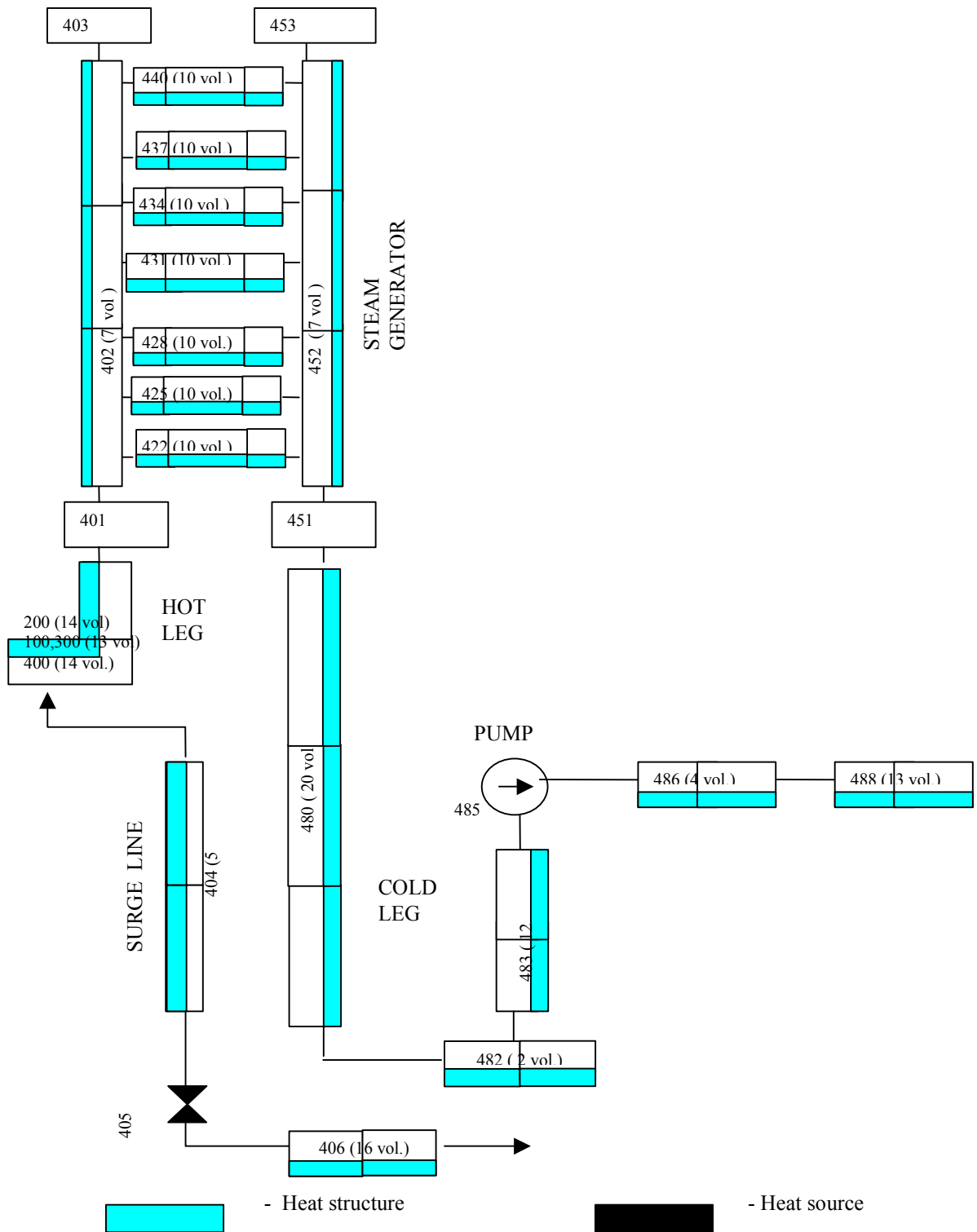


Figure 3. EREC nodalization of the intact loop.

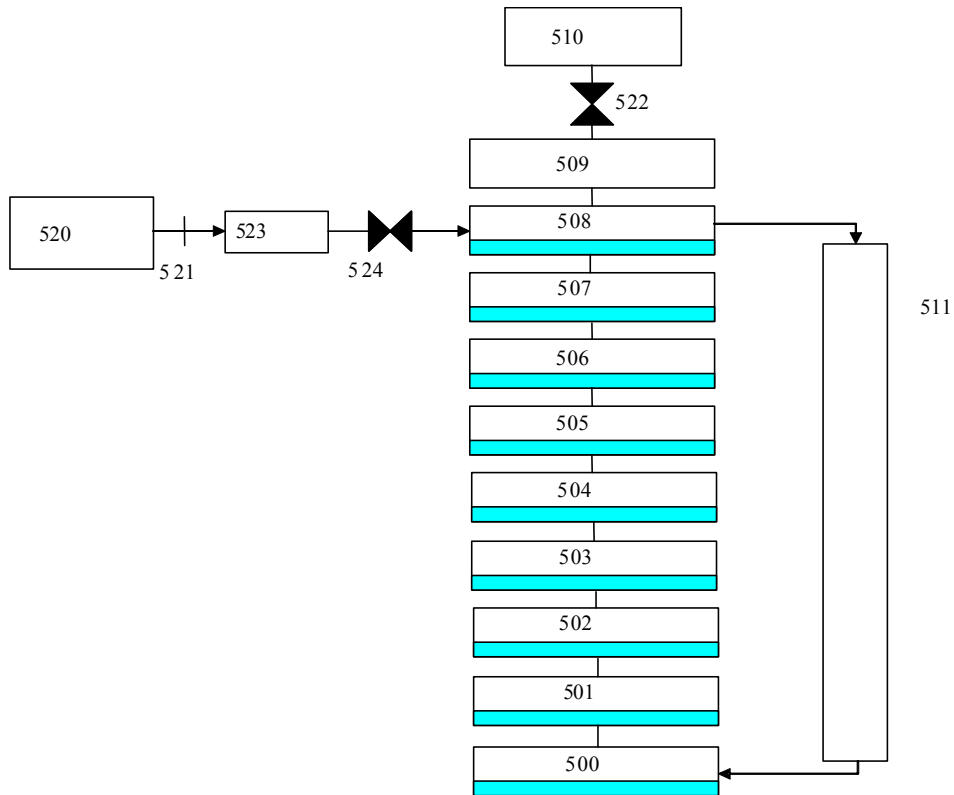


Figure 4. EREC nodalization of the secondary system.

While the two models were generally similar, there were some differences.

The major nodalization difference was in the modeling of the steam generators. The tube bundle was modeled with seven different levels in the EREC model, and with five levels in the INEEL model. The EREC model separated the downcomer region from the riser portion, while the INEEL model treated these as a single stack of volumes. The individual steam lines, relief valves, and the common steam header were included in the INEEL model, but not in the EREC model. These differences were not expected to be significant because the steam generators do not play an important role in the loss-of-coolant experiment being simulated.

The pump curves for the primary system pumps were different in the two models. With no data on the pumps in the experiment facility, EREC used typical VVER pump curves, while INEEL used the built-in data in the code for Westinghouse pumps. Since the primary coolant pumps trip early in the transient and coast down rapidly, the pumps should have little impact on the transient.

Flow through the core bypass is lower in the EREC model. The INEEL model adjusted the loss coefficients to match the core bypass outlet fluid temperature measurement during steady state, while the EREC model loss coefficients were not changed. The result

was much lower flow through the EREC model, with a coolant outlet temperature nearly 50 K higher than the INEEL model.

The EREC model had the countercurrent flow limitation (CCFL) model turned on at every junction in the core and upper plenum; the INEEL model had it on at only three locations: the core outlet, the junction below the hydroaccumulator injection, and the plate between the upper plenum and the upper head.

Other minor modeling differences included the pressurizer heaters, system heat losses, the line from the top of the downcomer to the upper plenum models differed.

Both input decks were run to steady state conditions prior to starting the transient calculations. The method used to achieve the initial conditions was different. In the EREC model, the steam generator pressures were controlled, and the primary coolant system temperatures were allowed to float, resulting in steady state loop temperatures that were higher than in the test. In the INEEL model, the steam header pressure was varied to get the specified cold leg temperature, resulting in steady state steam generator pressures that were lower than those in the test. Table 1 shows the major initial conditions calculated.

Simulation Results

Measured and calculated pressures in the upper plenum are presented in Figure 6. Table 2 provides the sequence of significant events for the experiment. A brief overview of the behavior observed in the experiment is provided here, then the comparisons between the data and calculations will be presented and discussed. Following the break opening, the system pressure decreased rapidly. The depressurization slowed near 50 s, as liquid began to boil in the core. As the pressure continued to decrease, hydroaccumulator injection began near 200 s. Condensation of some of the steam in the system by the cold ECC liquid caused the depressurization rate to increase. The ECC injection flow could not fully compensate for the break flow, allowing the core liquid level to drop low enough that the core began to heat up above the coolant saturation temperature. A cyclic behavior was then observed in the primary coolant system. The hydroaccumulator injection increased the depressurization rate because of steam condensing on the cold water being injected. This further increased the hydroaccumulator flow, refilling parts of the downcomer and core. As the liquid level in the core increased, the heater rods were quenched, and the increased vapor generation caused the pressure to increase, stopping hydroaccumulator injection. Without the hydroaccumulator injection, the liquid level in the core decreased, and the heater rods began to heat up again. The vapor generation rate was reduced because less liquid was available to boil, so the pressure decreased, allowing the hydroaccumulators to inject liquid again. This cyclic hydroaccumulator injection continued through much of the experiment, although the injection became less effective in stopping the core heatup; after 700 s, the injection was unable to completely quench the core. The test was terminated shortly after 1000 s to protect the heater rods, when the maximum heater rod temperature was near 1100 K.

Table 1. Measured and calculated steady state conditions.

Parameter	Experiment	EREC	INEEL
Upper plenum pressure (MPa)	16.9±0.06	16.9	16.9
Downcomer inlet temperature (K)	559.7±3	562.95	559.7
Upper plenum outlet temperature (K)	589.7±3	592.62	589.5
Core power (kW)	1520±15	1527	1520
Core bypass power (kW)	17.4±0.7	17.3	17.4
Pressurizer level ^a (m)	6.99±0.3	6.99	6.99
Loop flow (kg/s)			
Loop 1	2.3± 0,05	2.3	2.3
Loop 2	2.3± 0,05	2.3	2.3
Loop 3	2.3± 0,05	2.3	2.3
Loop 4	2.4± 0,05	2.4	2.4
Liquid level (m)			
Steam generator 1	1.71±0.07	1.74	1.71
Steam generator 2	1.71±0.07	1.74	1.71
Steam generator 3	1.84±0.07	1.88	1.84
Steam generator 4	1.74±0.07	1.75	1.74
Pressure (MPa)			
Steam generator 1	7.43±0.05	7.43	7.17
Steam generator 2	7.47±0.05	7.47	7.17
Steam generator 3	7.33±0.05	7.33	7.17
Steam generator 4	7.43±0.05	7.43	7.17
Liquid level (m)			
Hydroaccumulator 1	4.84± 0.07	4.84	4.83
Hydroaccumulator 2	4.84± 0.07	4.84	4.84
Hydroaccumulator 3	4.86± 0.07	4.86	4.86
Hydroaccumulator 4	4.85± 0.07	4.85	4.84
Pressure (MPa)			
Hydroaccumulator 1	5.8± 0.03	5.8	5.9
Hydroaccumulator 2	5.8± 0.03	5.9	6.0
Hydroaccumulator 3	5.9± 0.03	5.9	5.9
Hydroaccumulator 4	5.9± 0.03	5.9	5.9

a. The specified pressurizer level is the reading from measurement YP01L02, whose lower tap is 1.885 m above the bottom of the pressurizer.

The calculated pressure decreased a little more rapidly than was measured immediately after the break was opened, in both the EREC and INEEL calculations. The calculated depressurization rate is higher than measured when hydroaccumulator injection began. In the EREC calculation, the discrepancy at this stage is more pronounced than in the INEEL calculation. The INEEL and EREC calculations both qualitatively demonstrated the same effects of the periodical hydroaccumulator injection with the increasing of the depressurization rate at the beginning of the injection cycle and temporary repressurization at the end of the injection cycle.

Table 2. Measured and calculated sequence of events.

Event	Time (s)		
	Data	INEEL	EREC
Break opens	0	0	0
Scram/power decrease	5	5 ^a	5 ^a
Pressurizer heaters turned off	6	5	5
Main coolant pumps tripped	10	10 ^a	10 ^a
Steam generator 4 feedwater flow ends	10	10 ^a	15 ^a
Steam generator 1 feedwater flow ends	13	13 ^a	15 ^a
Steam generator 3 feedwater flow ends	14	14 ^a	15 ^a
Steam generator 2 steam flow ends	17	17 ^a	22 ^a
Pressurizer above heaters empties (measurement YP01L02)	19	16	16
Steam generator 1 steam flow ends	20	20 ^a	22 ^a
HPI starts	21	18	16
Steam generator 4 steam flow ends	23	23 ^a	22 ^a
Steam generator 3 steam flow ends	24	24 ^a	22 ^a
Primary pressure drops below secondary pressure	86	83	60
Hydroaccumulator 4 injection starts	165	163	149
Hydroaccumulator 2 injection starts	175	157	149
Hydroaccumulator 3 injection starts	184	163	149
Hydroaccumulator 1 injection starts	194	163	150
Core heatup starts	222	170	470
Core bypass heater tripped	559	--	560 ^a
Experiment terminated	1037	830	1050

a. Specified boundary condition in the calculation, based on the experiment data

Figure 7 shows the mass flow rate through the break. Despite the higher calculated peak flow rate, the calculations released about the same total mass through the break during the first 20 s. The calculated flow rates were then higher than the measured value for about 50 s, although the upstream fluid densities were the same; this is an indication that using a smaller discharge coefficient in the input model would provide a better match to the data. The calculated flows made the transition to a high quality mixture faster than the test, resulting in a lower flow rate from 100-300 s. The periodic hydroaccumulator injection had a more noticeable effect in the test than in the calculations, causing small increases in the mass flow rate as some of the liquid being injected into the upper plenum was entrained through the break.

Figure 8 presents the measured and calculated pressurizer levels, for the instrument that spans the portion of the pressurizer from just above the heaters to the top of the tank. This portion of the pressurizer drained slightly faster in the calculation than in the test, emptying at 16 s in both the EREC and INEEL calculations compared to 19 s in the experiment. Using a smaller break discharge coefficient, as mentioned above, would improve the draining comparison.

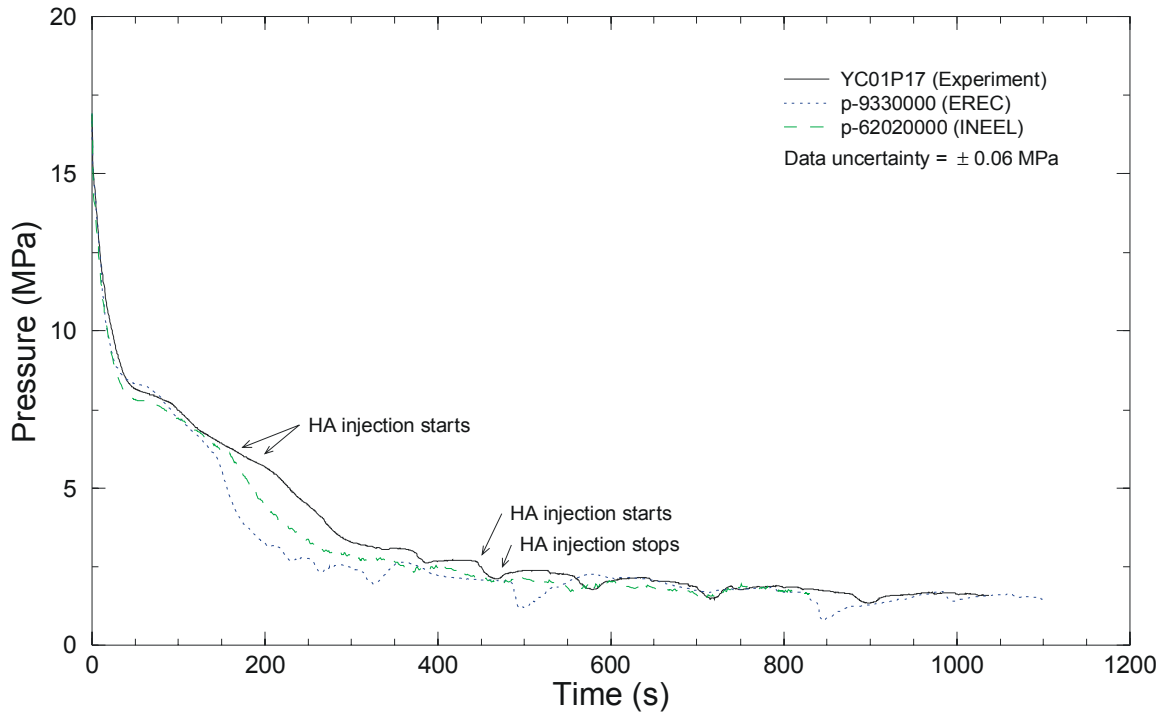


Figure 6. Upper plenum pressure.

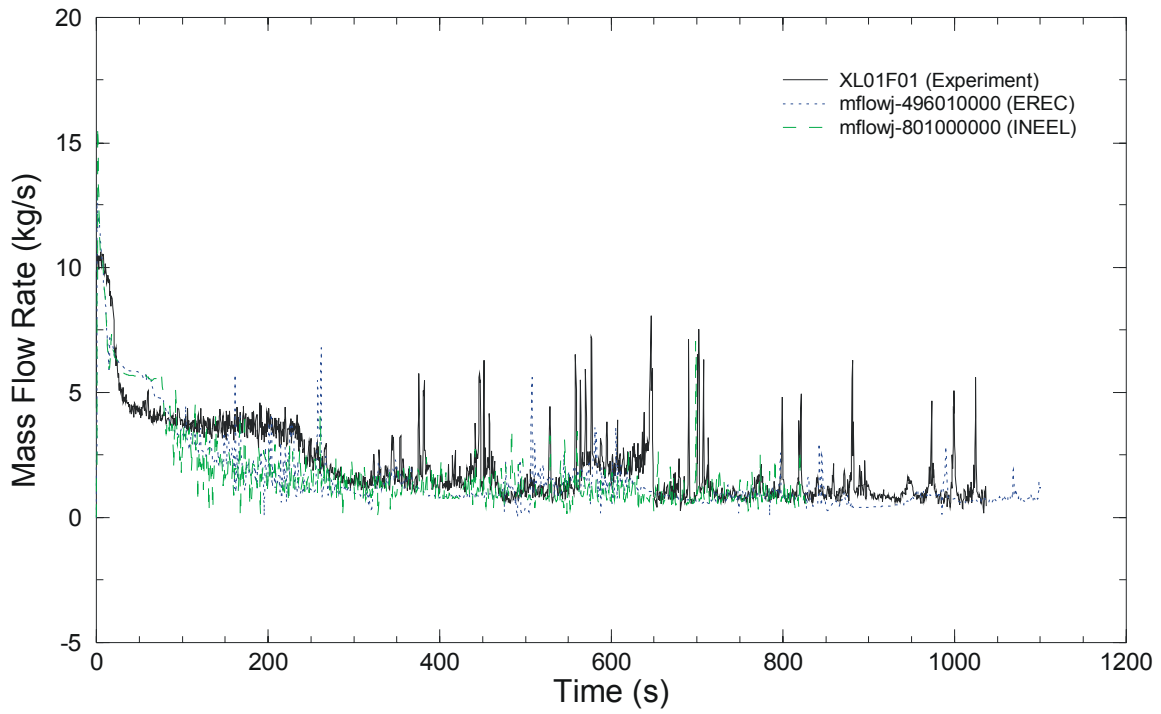


Figure 7. Break flow rate.

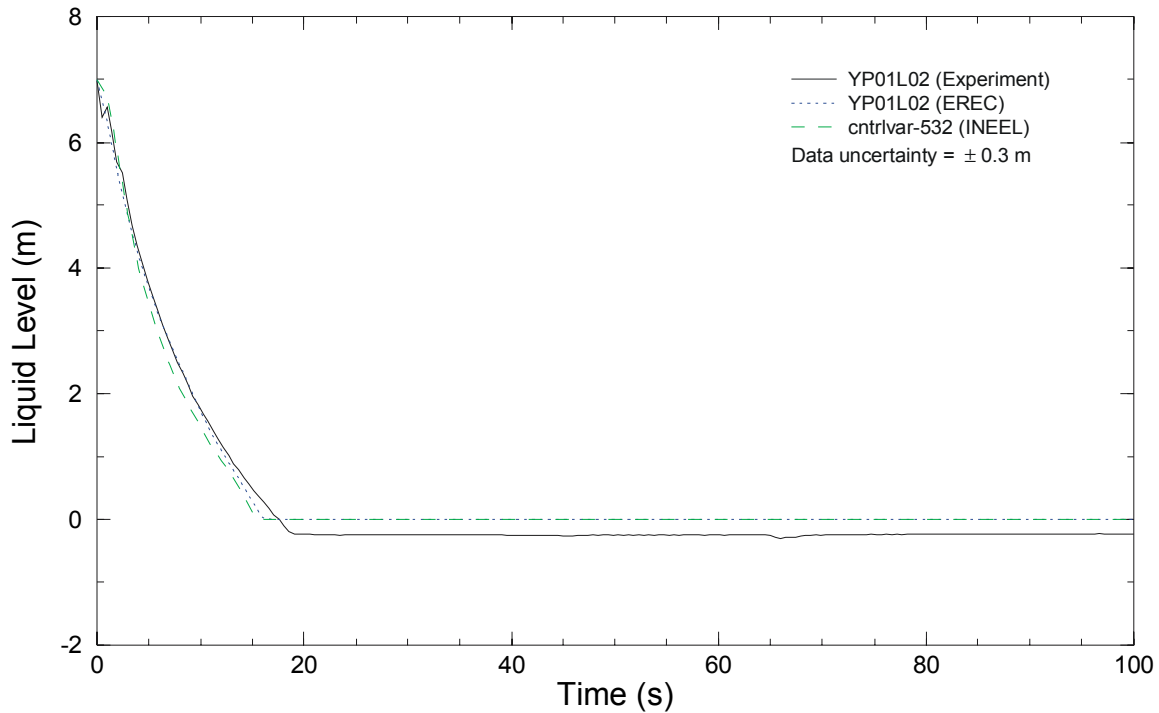


Figure 8. Pressurizer liquid level.

The liquid level and pressure in hydroaccumulator 1 are shown in Figures 9 and 10, respectively. As with the accumulator levels, the pressure reflects the periodic injection to the primary system, with the calculated pressure dropping earlier because of the lower calculated primary system pressure. The small increases in pressure between injections in the data were not captured in the calculation. The pressure increased because of heat transfer from the hotter walls to the vapor in the accumulator, an effect that was underpredicted by the code.

Differential pressures in different axial regions of the core are shown in Figures 11-13. The initial void formation in the core was reasonably simulated by the code in both calculations. In the experiment and the EREC calculation, the upper portion of the core had less liquid than the lower portions, while in INEEL calculation the axial void profile was fairly uniform. The effects of the hydroaccumulator injection were also different in the test and calculations. In the test, the beginning of the hydroaccumulator injection cycle resulted in decreases in the differential pressure after a short delay. After the injection stopped, the differential pressures in the upper and lower portions slowly moved toward their previous values, and the middle of the core saw a rapid increase to values above zero. Since the measurement should read slightly below zero when the region is steam filled, this may be an indication of a problem with the measurement. In general, the effect of the hydroaccumulator injection is not noticeable in the calculated differential pressure curves.

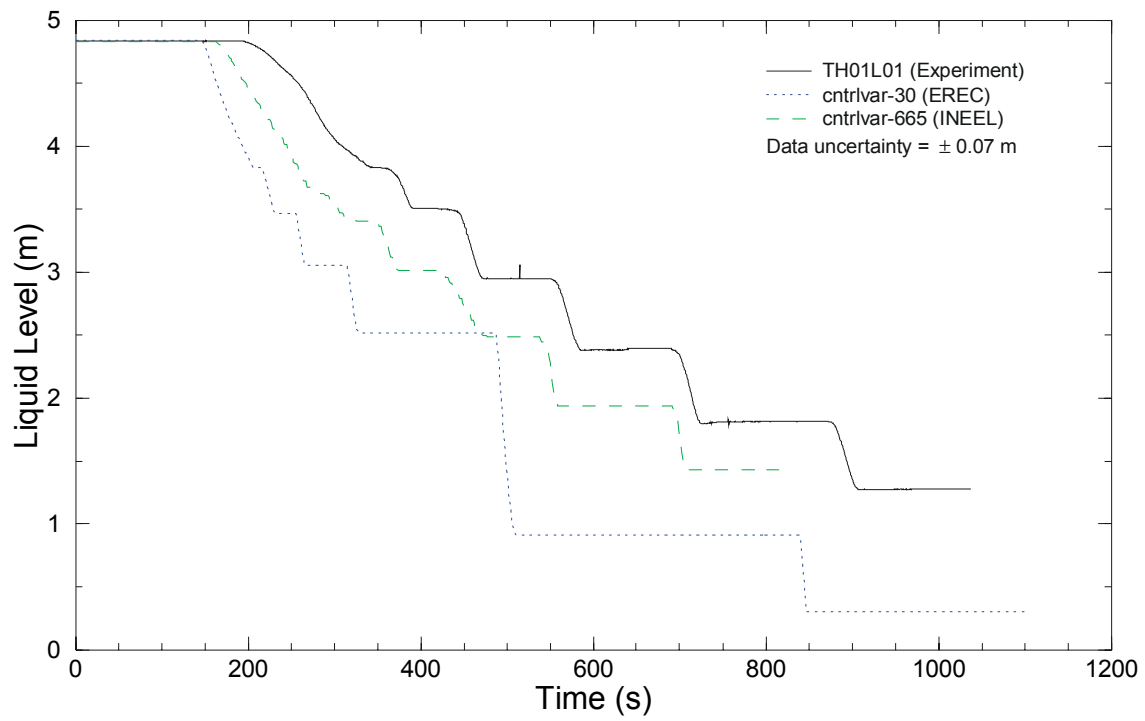


Figure 9. Hydroaccumulator 1 liquid level.

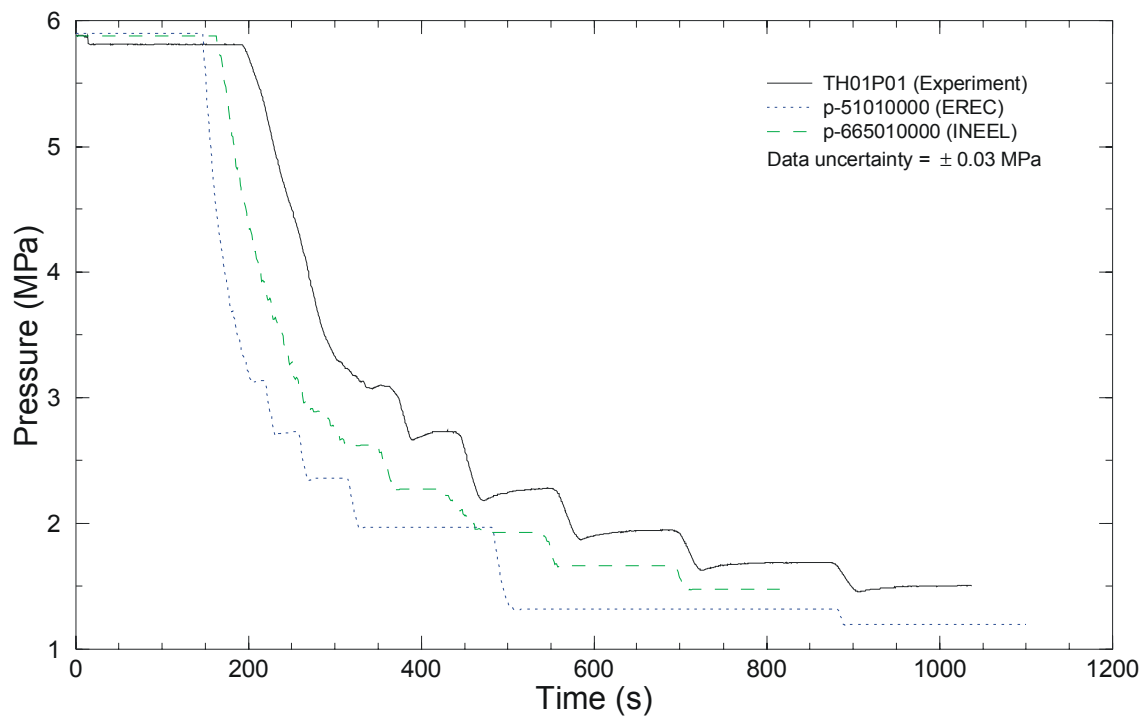


Figure 10. Hydroaccumulator 1 pressure.

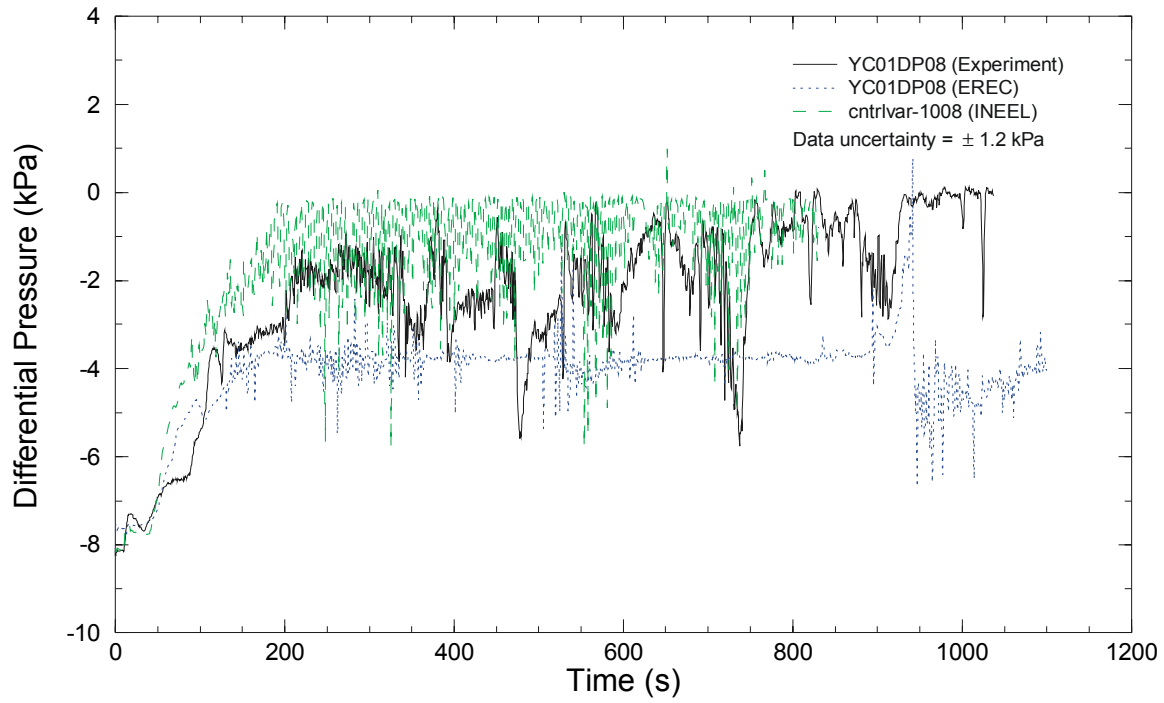


Figure 11. Differential pressure in the lower portion of the core simulator.

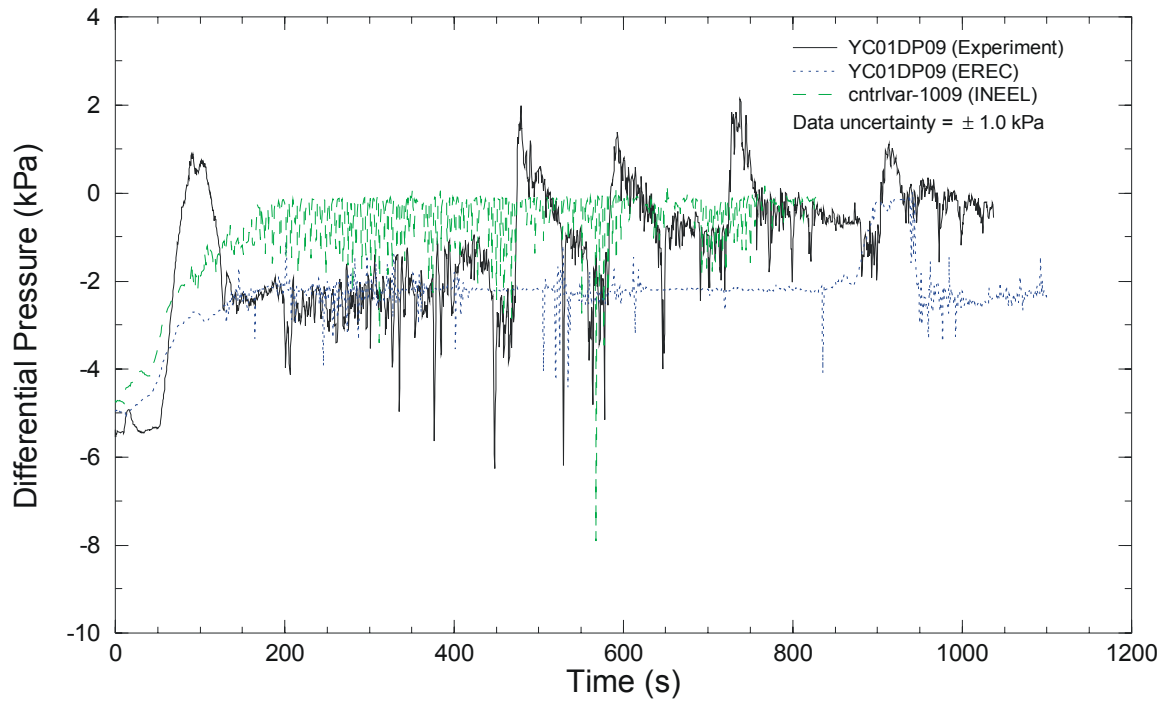


Figure 12. Differential pressure in the middle portion of the core simulator.

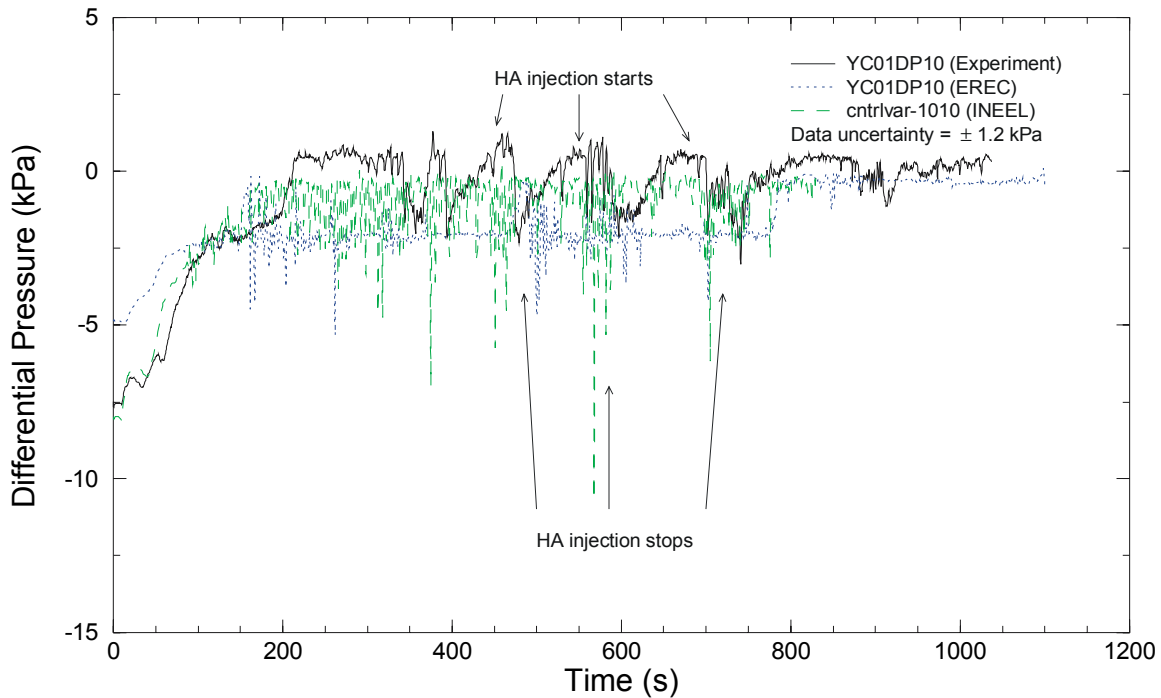


Figure 13. Differential pressure in the upper portion of the core simulator.

Measured and calculated fuel simulator cladding surface temperatures are shown in Figures 14-16. The data show a series of top-down core heatups that were terminated by hydroaccumulator injection, returning the cladding to the coolant saturation temperature. As the transient progressed, the hydroaccumulator injection became less effective in terminating the heatup, as more of the length of the heater rods became involved in the heatup. By the end of the transient, the hydroaccumulator injection could only partially cool (not quench) the core, and the heatup continued until the power was reduced to protect the heater rods.

In the INEEL calculation, the heatup started about 50 s earlier than in the test, because of the lower system pressure, and there were almost continuous small heatups of 20-30 K over the entire length of the core. While a greater portion of the core was involved than in the test, the heatups were not as extensive. Near 350 s, a more extensive heatup was calculated in the top portion of the core, which was subsequently quenched by hydroaccumulator injection. The next two periods of extended core heatup were only partially quenched by the hydroaccumulator injection, and the temperatures increased sufficiently that the INEEL calculation was terminated at 830 s.

The injection of the hydroaccumulator water was cyclic in the EREC calculation as in the INEEL calculation and experiment, but the frequency of the cyclic injection in the EREC calculation differed from that in the experiment and the INEEL calculation. The amount of water injected during an injection cycle in the EREC calculation was larger than the amount in the INEEL calculation and experiment. This resulted in only one heatup and

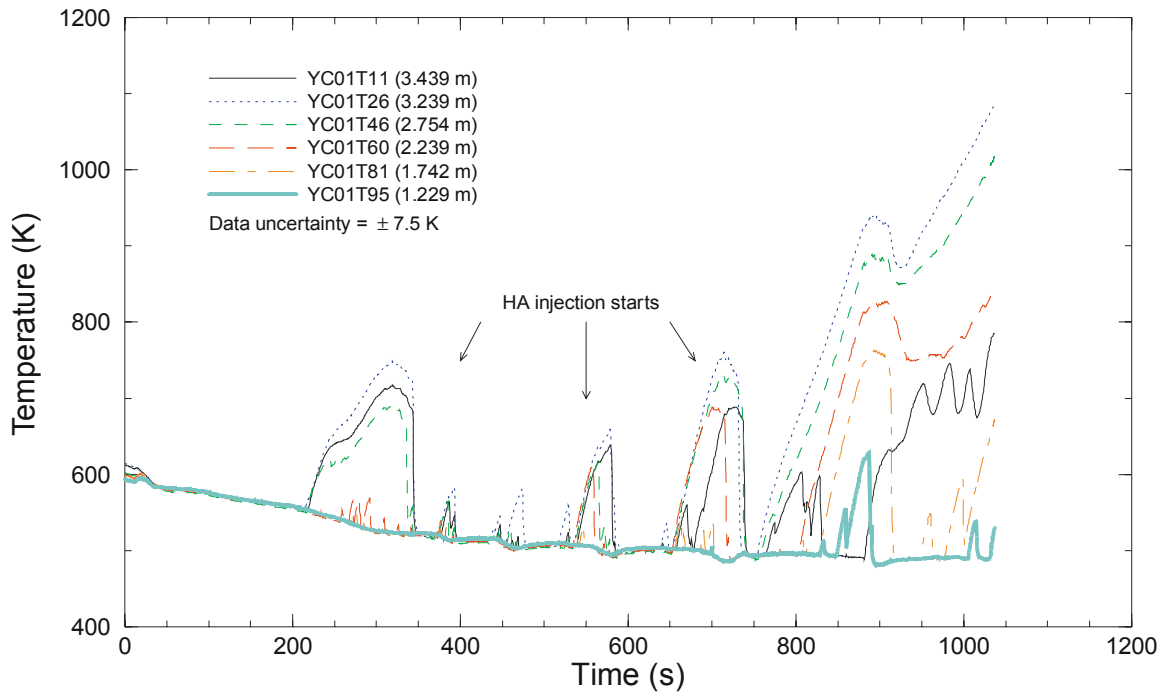


Figure 14. Measured heater rod surface temperatures.

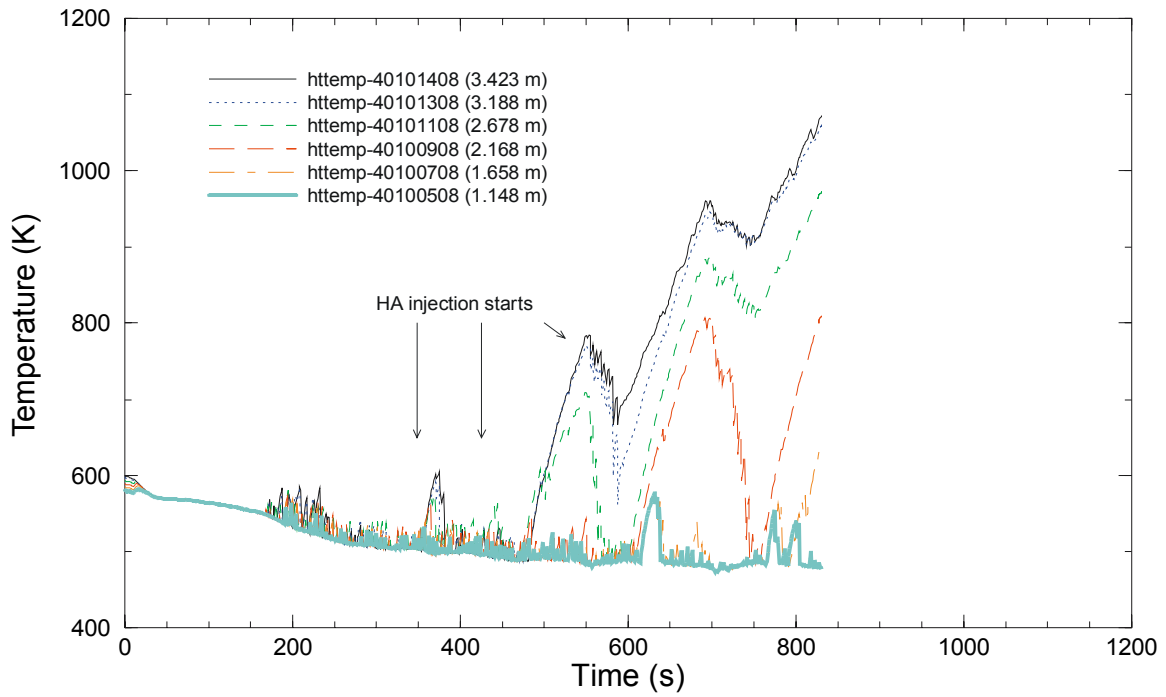


Figure 15. Heater rod surface temperatures from the INEEL calculation.

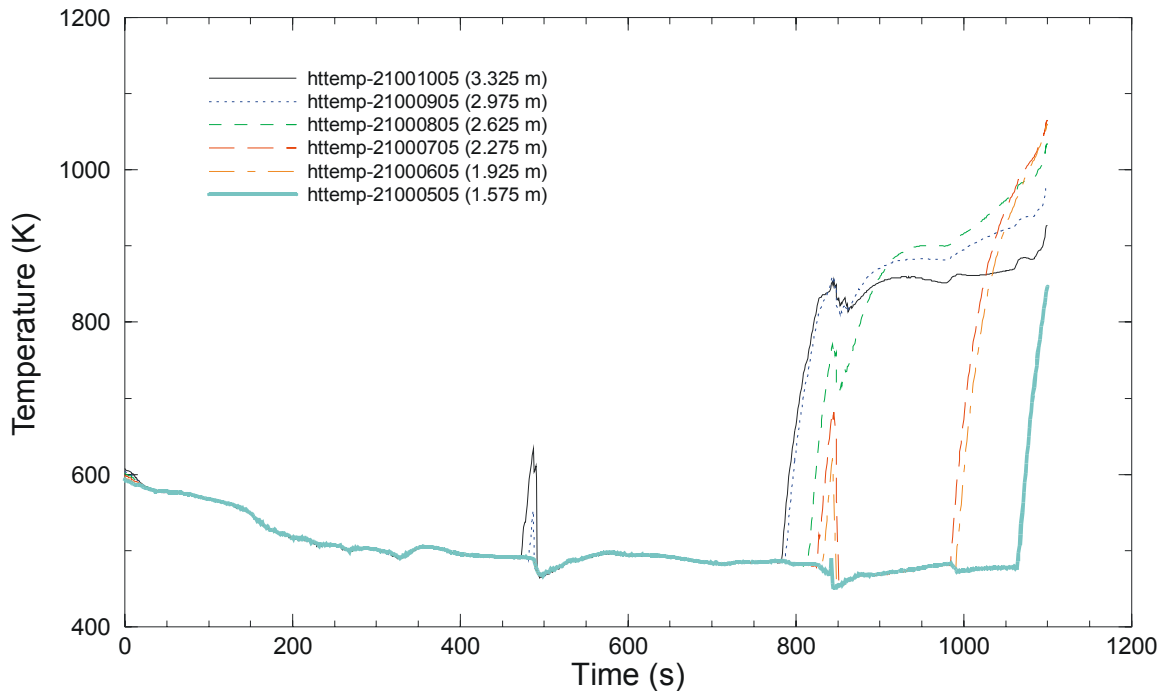


Figure 16. Heater rod surface temperatures from the EREC calculation.

quench cycle in the EREC calculation before the final heatup, while in the experiment and INEEL calculation several cycles of core heatup and quenching were observed.

The response of the top-most measured temperature near the end of the test suggests that there may have been some liquid entering the core from the upper plenum to partially cool the upper end of the heater rods. This was not predicted in the INEEL and EREC calculations, where the CCFL model was invoked at the core outlet junction more than 70% of the time after the core heatup began, often preventing liquid in the upper plenum from flowing down into the core. Measured temperatures near the top of the core from several different heater rods are shown in Figure 17, where it is seen that there is some radial variation in the temperatures. There are likely multi-dimensional effects in the experiment that allow some liquid penetration from the upper plenum into the core, but these cannot be captured with the one-dimensional nodalizations used in the RELAP5 models. The modeling of these processes requires two or more fuel rod channels in the core section. However, it is difficult to determine boundary conditions for cross flows between these parallel channels.

Conclusions and Recommendations

Table 3 presents the code assessment findings for the important phenomena identified as being addressed by this experiment. Most of the phenomena that were present in the test were reasonably simulated by the code. The major difference between the test and the calculation was the timing of the core heatup, and the thermal response to the hydroaccumulator injection cycles in both calculations.

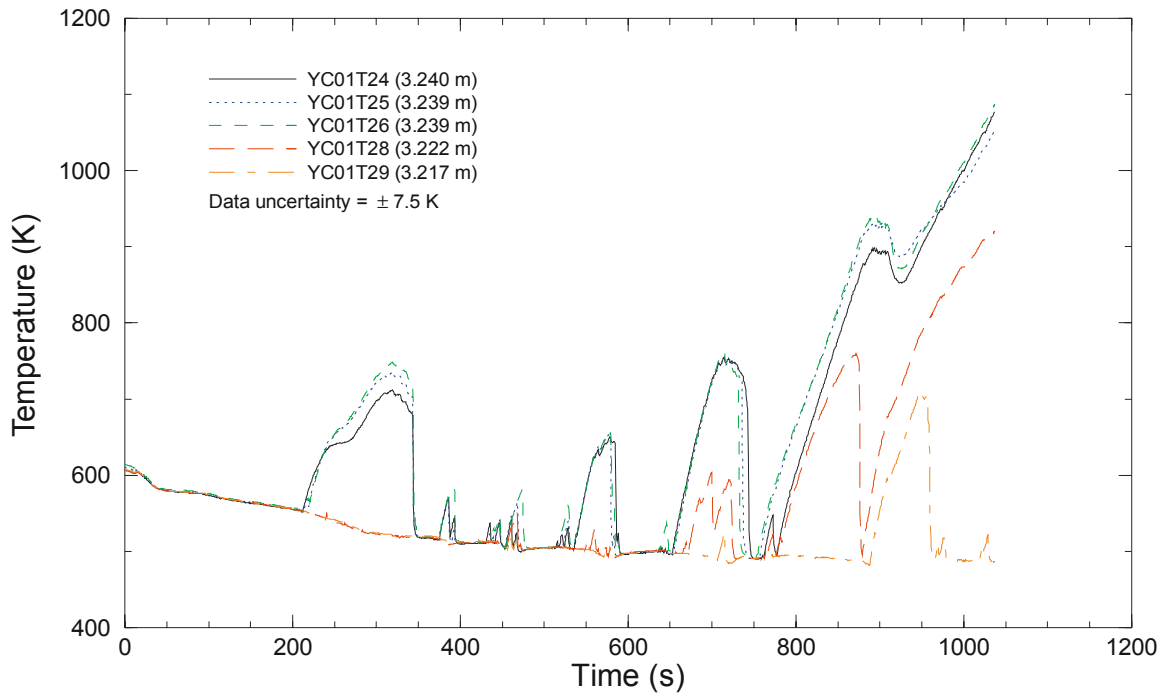


Figure 17. Measured heater rod temperatures near the top of the bundle.

The INEEL calculation had a more extensive axial heatup, with most of the core experiencing small heatups. The hydroaccumulator injection was more effective in quenching the core in the test than in the INEEL calculation. This difference is attributed to the liquid distribution in the core, rather than to the heat transfer models in the code. The code calculation had a more uniform axial distribution of the liquid in the core, and the hydroaccumulator injection did not have much impact on the core liquid inventory. Based on this, the code simulation of the mixture level and entrainment in the core was judged to be minimal.

In the EREC calculation, only one heatup of the cladding temperature was observed for upper and middle section of the fuel rods before the final heatup. The difference can be attributed to differences in liquid distribution, namely the core region in the EREC calculation contains more liquid over most of the transient than in the experiment. The distribution of liquid in the core in EREC calculation is also more uniform than in the experiment. Therefore, the code simulation of the mixture level and entrainment in the core was judged to be minimal.

Assessment judgments were not made for several phenomena in the INEEL and EREC analyses, either because they did not occur in the test or because there were insufficient measurements to characterize them.

An improved simulation of the core behavior was achieved in an INEEL sensitivity calculation in which the interphase drag in the core was increased by turning off the

Table 5.1. Assessment results for high-ranked phenomena.

Phenomenon	EREC judgment	INEEL judgment
Primary system two-phase natural circulation	Reasonable	Reasonable
Asymmetric loop behavior	Reasonable	Reasonable
Leak flow	Reasonable	Reasonable
Phase separation without mixture level formation	None made	None made
Mixture level and entrainment in the steam generator	None made	None made
Mixture level and entrainment in the core	Minimal	Minimal
Flow stratification in horizontal pipes	None made	None made
Loop seal clearance in the cold legs	Reasonable	Reasonable
Pool formation in the upper plenum	None made	None made
Heat transfer in a covered core	Reasonable	Reasonable
Heat transfer in a partially uncovered core	Reasonable	Reasonable
Pressurizer thermal-hydraulics	Reasonable	Reasonable
Integral system effects	Reasonable	Reasonable

bundle volume flag. The current user recommendation is to use the bundle flag in vertical rod bundles. These results suggest that that may not be appropriate for the VVER bundle geometry. However, this was only a single bundle, and the results may differ at full scale. Users should at least investigate the sensitivity of their results to the interphase drag modeling in the core.

References

1. The RELAP5 Code Development Team, "RELAP5/MOD3 Code Manual", NUREG/CR-5535 (INEL-95/0174), Volumes I-V, Idaho National Engineering Laboratory, Idaho Falls, Idaho (June 1995).
2. O. I. Melikhov, I. V. Elkin, I. A. Lipatov, G. I. Dremin, S. A. Galchanskaya, S. M. Nikonov, A. A. Rovnov, A. I. Antonova, E. Yu. Chtchepetilnikov, A. V. Kapustin, V. I. Gidkov, and A. F. Chalych, "Standard Problem Definition Report for INSCSP-PSBV1: 11% Upper Plenum Break", (Deliverable PV1-3 of Work Order 38 under Joint Project 6 with the U. S. International Nuclear Safety Center), International Nuclear Safety Center of Russian Minatom, Moscow, Russia (2002).
3. O. V. Gavritenkova, I. V. Parfenov, O. I. Melikhov, V. I. Melikhov, and P. D. Bayless, "Comparative Assessment of VVER Standard Problem INSC-PSBV1: 11% Coolant Leak from Upper Break", United States and Russian Minatom International Nuclear Safety Centers, Moscow, Russia and Idaho Falls, ID, USA (October 2003).